ACS APPLIED MATERIALS & INTERFACES

Research Article

www.acsami.org

N-Doped Amorphous Carbon Coated Fe_3O_4/SnO_2 Coaxial Nanofibers as a Binder-Free Self-Supported Electrode for Lithium Ion Batteries

Wenhe Xie, Suyuan Li, Suiyan Wang, Song Xue, Zhengjiao Liu, Xinyu Jiang, and Deyan He*

School of Physical Science and Technology, and Key Laboratory for Magnetism and Magnetic Materials of the Ministry of Education, Lanzhou University, Lanzhou 730000, China

Supporting Information

ABSTRACT: N-doped amorphous carbon coated Fe_3O_4/SnO_2 coaxial nanofibers were prepared via a facile approach. The core composite nanofibers were first made by electrospinning technology, then the shells were conformally coated using the chemical bath deposition and subsequent carbonization with polydopamine as a carbon source. When applied as a binder-free self-supported anode for lithium ion batteries, the coaxial nanofibers displayed an enhanced electrochemical storage capacity and excellent rate performance. The morphology of the interwoven nanofibers was maintained even after the rate cycle test. The superior electrochemical performance originates in the structural stability of the N-doped amorphous carbon shells formed by carbonizing polydopamine.

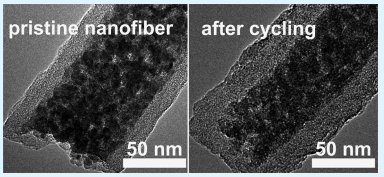

KEYWORDS: *Fe_3O_4/SnO_2, composite nanofibers, N-doped amorphous carbon coating, carbonized polydopamine, anode*

1. INTRODUCTION

Lithium ion batteries (LIBs) are widely applied to a variety of electronic products such as mobile phones, laptop computers, cameras, and so on. Although the current LIBs have many advantages compared with the other rechargeable batteries, they still cannot fully meet the growing energy storage demands. As we know, the anode material for most of the commercial LIBs is graphitic carbon; its lower theoretical specific capacity hinders a further improvement of the energy density and power density of the batteries. Therefore, various anode materials with higher theoretical specific capacities have been developed so far.[1,2]

Metal oxides have attracted great attention due to their high theoretical specific capacity.[3−9] However, their inherent low electronic conduction results in the poor cycling capabilities and the inferior rate performances. Moreover, they suffer from serious structural pulverization arising from the drastic volume changes during the lithium insertion/extraction processes, which can lead to the exfoliation from the current collector.

Many approaches have been developed to improve the electrochemical performance of the metal oxide electrodes,[10−14] Two of them are widely used. The one is to fabricate composites with carbonaceous materials, such as glucose[15] and graphene,[16,17] for increasing the electrical conductivity and buffering the volume change of the active metal oxides. Some N containing carbon sources, such as PPy[18] and dopamine,[19] were also used because it had been shown that the resultant N-doped carbon is of an enhanced electrical conductivity, and when the corresponding composite is applied to the electrode of LIBs, it can lower charge transfer and form more stable solid electrolyte interface (SEI) films.[20,21]

The other one is to prepare composite metal oxides based on the fact that the composite can deliver a high cycling capability. When one metal oxide reacts with lithium, the other may absorb the corresponding volume change or act as a conductive matrix. Hierarchical SnO_2/Fe_2O_3 heterostructures,[22] ZnO/SnO_2,[23] and NiO/ZnO[24] nanofibers have been fabricated as enhanced anode materials for LIBs. On the other hand, metal oxide composites directly grown on metal substrates, for example, SnO_2/Fe_2O_3 nanotube on stainless steel substrate[25] and Co_3O_4/Fe_2O_3 nanowires on Ti substrate,[26] have been reported as binder-free electrodes for LIBs. Regardless of their superior electrochemical performance, the active mass loadings of the electrodes are low and the synthesis routes are complicated. Simple fabrication of binder-free self-supported metal oxide composites with higher mass loading has been rarely reported, to the best of our knowledge.

In this work, we report a facile strategy to synthesize self-supported carbon coated Fe_3O_4/SnO_2 coaxial nanofiber blanket with a high areal density and large area. The precursor of Fe_2O_3/SnO_2 composite nanofiber was first prepared by electrospinning technology. Superior to the other fragile metal oxide nanofibers, the as-spun Fe_2O_3/SnO_2 composite nanofibers have flexibility as well as high mechanical strength, and their morphology was well reserved after being coated with dopamine. A N-doped amorphous carbon coated Fe_3O_4/SnO_2 coaxial nanofiber blanket was then obtained after carbonization in an argon atmosphere.

2. EXPERIMENTAL SECTION

2.1. Preparation of the Fe_2O_3/SnO_2 Composite Nanofibers (Fe_2O_3/SnO_2 NFs). Polyvinylpyrrolidone (PVP, M_w = 1 300 000 g/mol), *N*,*N*-dimethylformamide (DMF), $FeCl_2{\cdot}4H_2O$, and $SnCl_2{\cdot}2H_2O$ were supplied by Sigma-Aldrich Corporation. Dopamine hydrochloride was purchased from Aladdin. In a typical procedure, 0.265 g of $FeCl_2{\cdot}4H_2O$, 0.15 g of $SnCl_2{\cdot}2H_2O$ (with a Fe:Sn molar ratio of 2:1), and 0.3 g of PVP were dissolved in 2.4 g of DMF under vigorous magnetic stirring

Received: August 29, 2014
Accepted: November 7, 2014
Published: November 7, 2014

for several hours. Then the mixture was electrospun using a 25 gauge injection needle with a flow rate of 0.15 mL/h and an applied voltage of 15 kV. The distance between the needlepoint and the grounded collector of aluminum foil was 17 cm. Finally, the as-spun fibers were calcined in air at 500 °C for 4 h.

2.2. Fabrication of the Carbonized Polydopamine Coated Fe_3O_4/SnO_2 Coaxial Nanofibers (C-PDA-Fe_3O_4/SnO_2 NFs). Typically, 80 mg of prepared Fe_2O_3/SnO_2 composite nanofibers was added to 200 mL tris-buffer solution (pH = 8.5, the concentration of dopamine is 0.6 mg/mL),[21,27] and a uniform and stable air flow was injected into the bottom of the aqueous solution. The polymerization was proceeded for 2 h at room temperature, and the obtained nanofibers were washed several times with deionized water. Following the same procedure, the polymerization was repeated for three times. Finally, the polydopamine coated Fe_2O_3/SnO_2 composite nanofibers were calcined at 500 °C for 4 h in an argon atmosphere. It should be noted that neither stirring nor centrifugation were involved during the fabrication of the carbonized polydopamine coating.

2.3. Structural Characterization. The structure and morphology of the resultant nanofibers were characterized by X-ray powder diffraction (XRD, X'Pert Pro Philips, Cu Kα radiation, λ = 0.154 056 nm), field-emission scanning electron microscopy (FE-SEMS-4800, Hitachi) and transmission electron microscopy (TEM, FEI, Tecnai G2 F30). Thermal gravimetric analysis (TGA, Du Pont Instrument 1090B) was carried out to evaluate carbon content with a heating rate of 10 °C/min. X-ray photoelectron spectroscopy (XPS) analysis was performed on a Kratos AXIS Ultra DLD instrument with an Al Kα probe beam.

2.4. Cell Assembling and Tests. CR-2032 coin cells were assembled in a pure argon-filled glovebox using lithium foil as the counter and Celgard 2320 as the separator membrane. The obtained nanofiber blanket was used as a working electrode, and the active mass loading was about 1.2 mg/cm^2. The electrolyte was 1 M $LiPF_6$ dissolved in ethylene carbonate (EC):dimethyl carbonate (DEC):ethyl methyl carbonate (EMC) in a 1:1:1 volume ratio. Galvanostatic charge–discharge cycling and rate tests were carried out at room temperature using a multichannel battery tester (Neware BTS-610). Cyclic voltammetry (CV) curves were measured with an electrochemical workstation (CHI-660C).

3. RESULTS AND DISCUSSION

3.1. Structural Characterization and Analysis. Figure 1a,b shows SEM images of the prepared Fe_2O_3/SnO_2 composite nanofibers. It can be seen that the nanofibers are randomly distributed to form an interwoven network. The average diameter of the nanofibers is about 70 nm. After polydopamine coating and carbonization, as shown in Figure 1c,d, the average diameter of the nanofibers increases to about 90 nm, while the interwoven network structure is still maintained. A similar structure of Fe_3O_4/SnO_2 and SnO_2 nanofibers is shown in Figure S1 (Supporting Information). Such an architecture constructs a convenient transport network for electrons, which is a benefit for the electrochemical reaction, as the material is used as an anode for LIBs. The optical image shown in Figure 1e illustrates that the large-areal nanofiber blanket is reserved after the fabrication of the carbonized polydopamine coating on Fe_3O_4/SnO_2 composite nanofibers, whereas its color changes from brown to black.

The TEM images in Figure 2a,b show the morphology of a single Fe_2O_3/SnO_2 composite nanofiber. It can be seen that the nanofiber consists of numerous interconnected nanoparticles and nanopores, which originated from chloride calcination and PVP decomposition in the air, respectively. The ultrafine particles prevent the metal oxides from aggregation. On the other hand, the nanopores are important for buffering volume change of the metal oxides during the lithiation/delithiation processes. Besides, the structure of the ultrafine nanoparticles and nanopores enhance the specific surface area of the nanofibers and facilitate the penetration of the electrolyte.

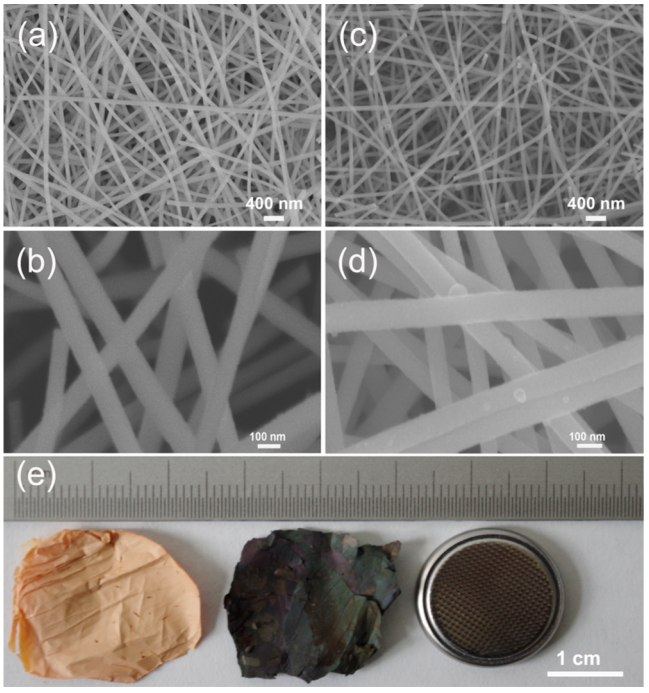

Figure 1. (a, b) SEM images of the prepared Fe_2O_3/SnO_2 composite nanofibers. (c, d) SEM images of the carbonized polydopamine coated Fe_3O_4/SnO_2 coaxial nanofibers. (e) Optical images of the nanofiber blankets and the assembled CR-2032 cell.

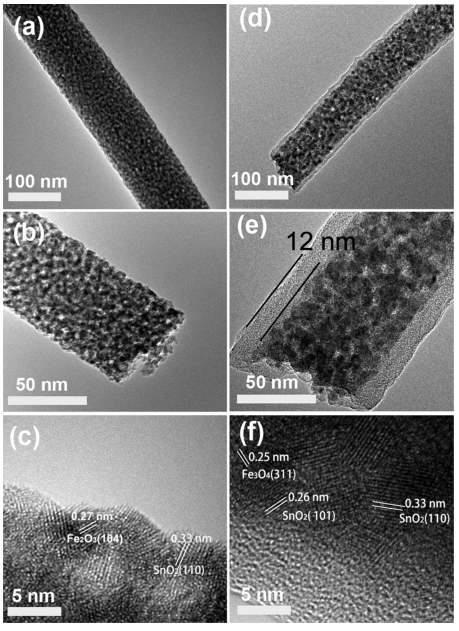

Figure 2. (a, b) TEM and (c) high-resolution TEM images of the prepared single Fe_2O_3/SnO_2 composite nanofiber. (d, e) TEM and (f) high-resolution TEM images of the carbonized polydopamine coated single Fe_3O_4/SnO_2 coaxial nanofiber.

It can be clearly seen from the TEM image shown in Figure 2d that the ultrafine nanoparticles and nanopores were maintained after the polydopamine carbonization. The average pore diameters in the Fe_2O_3/SnO_2 composite nanofiber and carbonized polydopamine Fe_3O_4/SnO_2 coaxial nanofiber are 5.44 and 4.55 nm, as shown in Figure S2 (Supporting Information). The carbonized polydopamine shell with a

thickness of 12 nm is obvious, as shown in Figure 2e. From the high-resolution TEM images shown in Figure 2c,f, the spacing of 0.33 nm can be found, which corresponds with the (110) planes of SnO_2 crystals, indicating that SnO_2 has not been reduced during the polydopamine carbonization. However, the spacing of 0.27 nm decreased to 0.25 nm after the polydopamine carbonization, indicating that Fe_2O_3 converted to Fe_3O_4. The TEM mapping shown in Figure S3 (Supporting Information) suggests that the elements of Fe, Sn, O, C, and N have a uniform distribution in the nanofiber.[28,29]

XRD measurement was carried out to identify the phase composition of the carbonized polydopamine coated Fe_3O_4/SnO_2 coaxial nanofibers. As shown in Figure 3a, the peaks at

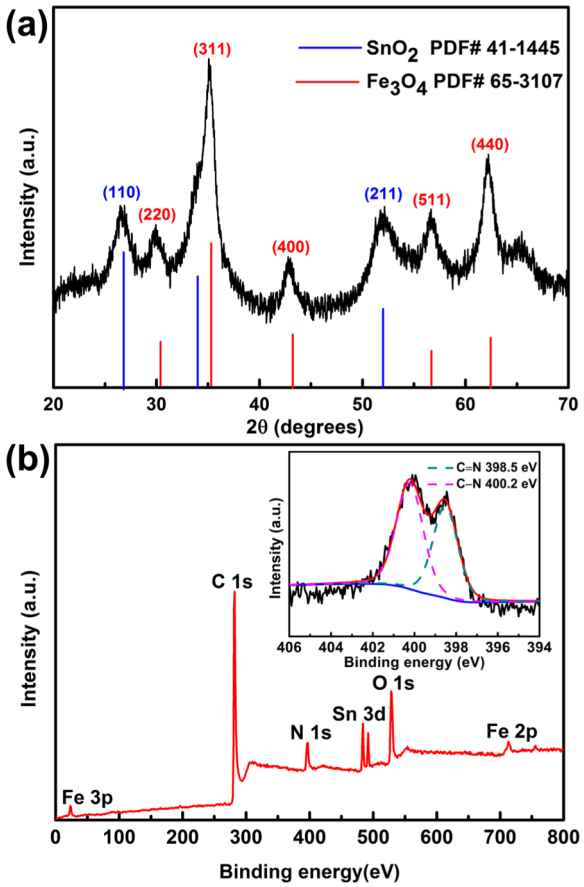

Figure 3. (a) XRD pattern and (b) XPS spectrum of the carbonized polydopamine coated Fe_3O_4/SnO_2 coaxial nanofibers. The insert in (b) is the high-resolution XPS spectrum of N 1s in the carbonized polydopamine shells.

26.6° and 51.8° are in good accordance with the diffraction from the (110) and (211) planes of SnO_2 (JCPDS 41-1445), respectively. The other peaks correspond to the diffraction from Fe_3O_4 (JCPDS 65-3107),[21] although all the peak positions shift to the lower angle less than 0.2° compared to the standard values, the XRD patterns of the composite nanofibers without carbon coating confirm that the majority of Fe_2O_3 transformed to Fe_3O_4 during the calcination at 500 °C in an argon atmosphere, as shown in Figure S4 (Supporting Information). The broaden peaks in the XRD patterns indicate that the sizes of the nanoparticles are fine. The fact that no peaks of carbon can be observed suggests that the carbonized polydopamine is amorphous.

A full XPS spectrum for a sample of the carbonized polydopamine coated Fe_3O_4/SnO_2 coaxial nanofibers is shown in Figure 3b, which clearly proves the presence of C, N, O, Fe, and Sn elements. The inset in Figure 3b is a high-resolution XPS spectrum of N 1s in the carbonized polydopamine, which corresponds to the C—N (pyrrolic nitrogen) structure at a binding energy of 400.2 eV and the C═N (pyridinic nitrogen) structure at 398.5 eV,[21] The evaluated N content incorporated in carbon shell is about 7.3 wt % based on the XPS measurement.

TGA analysis was conducted to quantify the mass percentage of the formed carbon shell on the nanofibers. As shown in Figure 4, a 4 wt % weight loss is observed before 300 °C, which can be

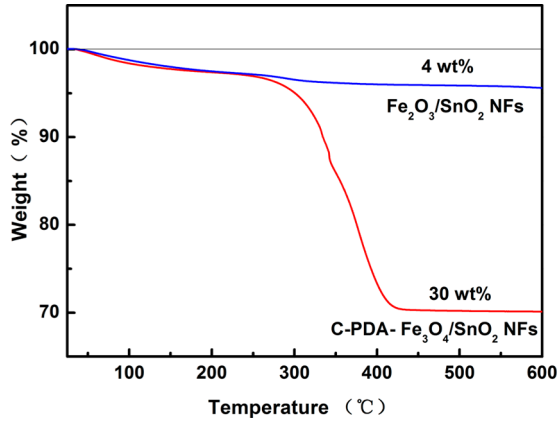

Figure 4. TGA profiles of the Fe_2O_3/SnO_2 composite nanofibers and the carbonized polydopamine coated Fe_3O_4/SnO_2 coaxial nanofibers.

attributed to the gas or water desorption from the porous structures. In the case of the carbonized polydopamine coated Fe_3O_4/SnO_2 coaxial nanofibers, a sharp drop ranging from 300 to 420 °C can be ascribed to the gas desorption and the combustion of carbon, which takes up 30 wt % of the composite. So, the mass percentage of carbon is 26 wt %. Assuming that the proportion of iron and tin in the resultant composite is same as their molar ratios in the precursor solution, the mass percentages of Fe_3O_4 and SnO_2 can be estimated to be 37.4 and 36.6 wt %, respectively. Thus, the calculated theoretical capacity of the composite is about 733 mAh/g. The TGA curve is almost horizontal in the subsequent heating process, suggesting that there are few low valence metal oxides or metal remaining in the nanofibers, which is consistent with the result of the XRD measurement.

3.2. Electrochemical Evaluation. Various experimental tests were conducted to analyze the electrochemical performance of the prepared nanofibers. As shown in Figure 5a, for the carbonized polydopamine coated Fe_3O_4/SnO_2 coaxial nanofibers, CV curves were measured under voltages ranging from 0.02 to 3.0 V vs Li^+/Li with a scan rate of 0.1 mV/s. A broad peak around 0.5 V is observed only in the first cathodic scan, which can be attributed to the irreversible formation of solid electrolyte interface (SEI) layer and the conversion of Fe_3O_4 to Fe. The reduction peak of Fe_3O_4 is located at 0.72 V in the subsequent cycles.[21] The relatively low potential peak near 0.1 V appear in all the cathodic scans, which corresponds to the alloying of Li_xSn. In the oxidation scans, two characteristic oxidation peaks located at 0.6 and 1.9 V correspond to the reversible dealloying of Li_xSn and the generation of Fe_3O_4, respectively.[21,30] The oxidation plateau located at 1.3 V implies partial reversible formation of SnO_2.[18] On the basis of the above CV analysis, the electrochemical

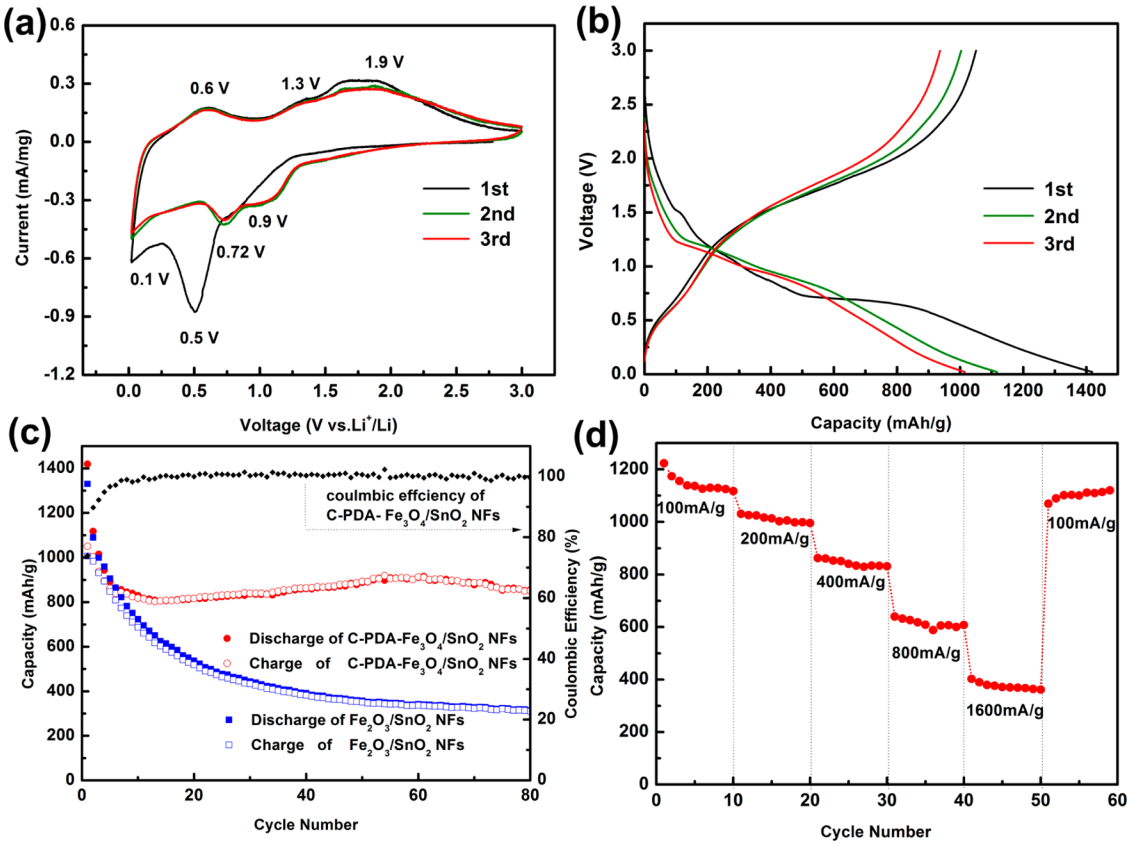

Figure 5. (a) Cyclic voltammetry curves and (b) charge−discharge profiles of the carbonized polydopamine coated Fe_3O_4/SnO_2 coaxial nanofiber electrode for the initial three cycles at a scan rate of 0.1 mV/s. (c) Cycling performances of the Fe_2O_3/SnO_2 composite nanofiber and the carbonized polydopamine coated Fe_3O_4/SnO_2 coaxial nanofiber electrodes at a current density of 100 mA/g. (d) Rate performance of the carbonized polydopamine coated Fe_3O_4/SnO_2 coaxial nanofiber electrode at various current densities.

reactions of the carbonized polydopamine coated Fe_3O_4/SnO_2 coaxial nanofibers can be described as follows

$$SnO_2 + 4Li^+ + 4e^- \rightarrow Sn + 2Li_2O \quad (1)$$

$$Sn + xLi^+ + xe^- \leftrightarrow Li_xSn\ (0 \le x \le 4.4) \quad (2)$$

$$Fe_3O_4 + 8Li^+ + 8e^- \leftrightarrow 3Fe + 4Li_2O \quad (3)$$

Figure 5b shows the initial three charge−discharge curves of the carbonized polydopamine coated Fe_3O_4/SnO_2 coaxial nanofiber electrode at a current density of 100 mA/g. The initial discharge and charge capacities are 1420 and 1051 mA/g, respectively. The initial capacity loss can be mainly attributed to the formation of SEI film and the irreversible reduction of SnO_2 as described by eq 1. Two obvious plateaus can be observed at 0.6 and 1.9 V in the charge profiles, which stand for the reversible dealloying of Li_xSn and the generation of Fe_3O_4.

The cyclic performance of the carbonized polydopamine coated Fe_3O_4/SnO_2 coaxial nanofiber electrode was measured under a constant current density of 100 mA/g. As a comparison, the cyclability of the Fe_2O_3/SnO_2 composite nanofiber electrode and the other nanofiber electrode were measured under the same current density as shown in Figures 5c and S5 (Supporting Information). It can be seen from Figure 5c that, in the initial several cycles, the charge−discharge capacities for the two nanofiber electrodes are almost overlapping. However, the capacity of the Fe_2O_3/SnO_2 composite nanofiber electrode decayed to 310 mAh/g in the subsequent cycles. On the other hand, after initial decaying to 810 mAh/g, the carbonized polydopamine coated Fe_3O_4/SnO_2 coaxial nanofiber electrode recovers and maintains at a high reversible capacity in the subsequent cycles. It delivers a reversible capacity of 850 mAh/g after 80 cycles, which is approximately 20% higher than the theoretical capacity. Most researchers attributed the enhanced reversible capacity of the metal oxide electrodes to the growth of polymeric gel-like film originating from the decomposition of electrolyte.[12,24,31] The Coulomb efficiency of the carbonized polydopamine coated Fe_3O_4/SnO_2 coaxial nanofiber electrode is higher than 96% after the fifth cycle onward.

The rate performance ranging from 100 to 1600 mA/g is shown in Figure 5d. The carbonized polydopamine coated Fe_3O_4/SnO_2 coaxial nanofiber electrode delivers high capacities of 1223, 1030, 862, and 640 mAh/g at 100, 200, 400, and 800 mA/g, respectively. Even after the current density is increased to 1600 mA/g, it still maintains a high charge capacity of 402 mAh/g. When the current density is restored to the initial setting of 100 mA/g, the carbonized polydopamine coated Fe_3O_4/SnO_2 coaxial nanofiber electrode leads to a reversible capacity of 1070 mAh/g. The above results suggest that the binder-free and self-supported electrode of the carbonized polydopamine coated Fe_3O_4/SnO_2 coaxial nanofibers displays superior a capacity retention as an well as excellent capacity recovery performance.

The superior electrochemical performance of the carbonized polydopamine coated Fe_3O_4/SnO_2 coaxial nanofibers comes from the design of the unique nanostructure. The structure and morphology of the carbonized polydopamine coated Fe_3O_4/SnO_2 coaxial nanofiber electrode after rate performance test were characterized by SEM and TEM. The SEM image in Figure 6a

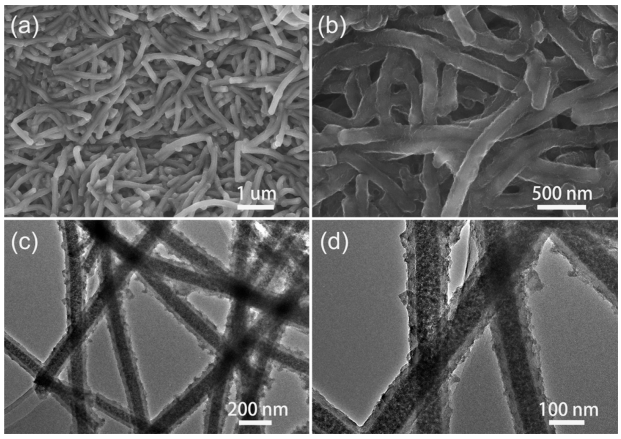

Figure 6. (a, b) SEM and (c, d) TEM images of the carbonized polydopamine coated Fe_3O_4/SnO_2 coaxial nanofibers after rate performance test.

shows that most of the nanofibers broke up into about 2 μm long fibers after enduring various current densities, which can be attributed to the mechanical stress from the cell assembling and the huge tension from the volume changes during the charge and discharge process. However, the nanofibers have not been pulverized because the volume change of the inner metal oxides is limited by the outer carbon shell. Besides, the broken nanofibers wrap to a three-dimensional network, as shown in Figure 6b. Such a three-dimensional network provides a better conductive channel and prevents the nanofibers from a further fragmentation during the electrochemical reactions. The TEM images in Figure 6c,d clearly show that the nanofibers were well maintained and firmly intertwined even after charge−discharge cycles at various current densities as well as the intense ultrasonic treatment in alcohol for washing of the remaining electrolyte. The thickness of the carbon shell increases to 22 nm from the HRTEM images shown in Figure S6 (Supporting Information), and the surface of the nanofibers becomes rougher significantly, as seen in the SEM and TEM images shown in Figures 1 and 2 before the electrochemical test, which may be attributed to the volume expansion, the formation of SEI layer, and the growth of the polymeric gel-like films.[32,33] The carbon coated nanofibers after constant current charge−discharge were well maintained, as shown in Figure S7 (Supporting Information).

The enhanced lithium storage performance of the carbonized polydopamine coated Fe_3O_4/SnO_2 coaxial nanofiber electrode can be concluded as follows. First, the interwoven blanket structure is well reserved during the polydopamine carbonization, which facilitates electronic conduction and lithium ion diffusion as evaluated from electrochemical impedance spectroscopy measurement, shown in Figure S8 (Supporting Information). Second, the porous metal oxides are encapsulated in the carbon shell, which accommodates huge volume change of the metal oxides and prevents the electrode from pulverization. Third, Fe and Sn are alternately generated due to their different charging and discharging plateaus. In the discharge process, Fe_3O_4 nanoparticles react with lithium while Sn acts as a conductive matrix, then the generated Fe and Li_2O serve as a conductive matrix while Sn reacts with lithium, and vice versa in the charge process. Such a mechanism promotes the electrochemical reaction and buffers the volume change. Besides, Fe and Sn nanoparticles facilitate the decomposition of electrolyte due to their catalytic activities.[24,34] Finally, as a result of N-doping, the carbonized polydopamine shell enhances the lithium storage performance.[19,35,36]

4. CONCLUSIONS

We have developed a simple method to fabricate N-doped amorphous carbon coated Fe_3O_4/SnO_2 coaxial nanofibers for application to anode of LIBs. The precursors of the Fe_2O_3/SnO_2 composite nanofibers were prepared by electrospinning technology, and the N-doped amorphous carbon shell was conformally coated using a chemical bath deposition and subsequent carbonization with polydopamine as a carbon source. The approach does not require complex operations or sophisticated equipment. The carbonized polydopamine coated Fe_3O_4/SnO_2 coaxial nanofiber electrode displays a high reversible capacity of 850 mAh/g after 80 cycles at a current density of 100 mA/g. It delivers reversible capacities of 1030, 862, 640, and 402 mAh/g at current densities of 200, 400, 800, and 1600 mA/g, respectively. When the current density resumes to 100 mA/g, the electrode reaches a satisfactory capacity of 1070 mAh/g. It is highlighted that the electrode structure was well maintained after the rate performance test, indicating that such an architectonic design can withstand a variety of harsh conditions. The excellent cycle performance and superior rate performance make the carbonized polydopamine coated Fe_3O_4/SnO_2 coaxial nanofibers an ideal candidate anode material for next-generation LIBs.

■ ASSOCIATED CONTENT

Ⓢ Supporting Information

SEM images of (a) the Fe_3O4/SnO_2 nanofibers and (b) the pure SnO_2 nanofibers, N_2 adsorption/desorption isotherms and the corresponding BJH distributions, TEM elemental maps of the carbonized polydopamine coated Fe_3O_4/SnO_2 coaxial nanofibers, XRD patterns of the Fe_2O_3/SnO_2 composite nanofibers, the Fe_3O_4/SnO_2 composite nanofibers and the pure SnO_2 nanofibers, cycling performances of the carbonized polydopamine coated Fe_3O_4/SnO_2 coaxial nanofibers, TEM and HRTEM images of a single nanofiber after the rate performance test, SEM image of the carbonized polydopamine coated Fe_3O_4/SnO_2 coaxial nanofibers after cycling, and Nyquist plots of the carbonized polydopamine coated Fe_3O_4/SnO_2 coaxial nanofiber, the Fe_2O_3/SnO_2 composite nanofiber, and the Fe_3O_4/SnO_2 nanofiber electrodes after the first cycle. This material is available free of charge via the Internet at http://pubs.acs.org.

■ AUTHOR INFORMATION

Corresponding Author

*D. He. E-mail: hedy@lzu.edu.cn. Fax: +86-931-8913554. Tel: +86-931-8912546.

Notes

The authors declare no competing financial interest.

■ ACKNOWLEDGMENTS

This project was financially supported by the National Science Foundation of China (grant no. 11179038) and the Specialized Research Fund for the Doctoral Program of Higher Education (grant no. 20120211130005).

■ REFERENCES

(1) Li, H.; Wang, Z.; Chen, L.; Huang, X. Research on Advanced Materials for Li-Ion Batteries. *Adv. Mater.* **2009**, *21*, 4593−4607.

(2) Zhou, X.; Yin, Y.; Cao, A.; Wan, L.; Guo, Y. Efficient 3D Conducting Networks Built by Graphene Sheets and Carbon Nanoparticles for High-Performance Silicon Anode. *ACS Appl. Mater. Interfaces* **2012**, *4*, 2824−2828.
(3) Poizot, P.; Laruelle, S.; Grugeon, S.; Dupont, L.; Tarascon, J. M. Nano-sized Transition-Metal Oxides as Negative-Electrode Materials for Lithium-Ion Batteries. *Nature* **2000**, *407*, 496−499.
(4) Wu, H. B.; Chen, J. S.; Hng, H. H.; Lou, X. W. Nanostructured Metal Oxide-based Materials as Advanced Anodes for Lithium-Ion Batteries. *Nanoscale* **2012**, *4*, 2526−2542.
(5) Li, D.; Li, X.; Wang, S.; Zheng, Y.; Qiao, L.; He, D. Carbon-Wrapped Fe_3O_4 Nanoparticle Films Grown on Nickel Foam as Binder-Free Anodes for High-Rate and Long-Life Lithium Storage. *ACS Appl. Mater. Interfaces* **2013**, *6*, 648−654.
(6) Li, Y.; Tan, B.; Wu, Y. Mesoporous Co_3O_4 Nanowire Arrays for Lithium Ion Batteries with High Capacity and Rate Capability. *Nano Lett.* **2007**, *8*, 265−270.
(7) Li, Y.; Tan, B.; Wu, Y. Freestanding Mesoporous Quasi-Single-Crystalline Co_3O_4 Nanowire Arrays. *J. Am. Chem. Soc.* **2006**, *128*, 14258−14259.
(8) Stromberg, J. R.; Wnuk, J. D.; Pinlac, R. A. F.; Meyer, G. J. Multielectron Transfer at Heme-Functionalized Nanocrystalline TiO_2: Reductive Dechlorination of DDT and CCl_4 Forms Stable Carbene Compounds. *Nano Lett.* **2006**, *6*, 1284−1286.
(9) Sun, X.; Si, W.; Liu, X.; Deng, J.; Xi, L.; Liu, L.; Yan, C.; Schmidt, O. G. Multifunctional Ni/NiO Hybrid Nanomembranes as Anode Materials for High-Rate Li-Ion Batteries. *Nano Energy* **2014**, *9*, 168−175.
(10) Nam, K. T.; Kim, D.-W.; Yoo, P. J.; Chiang, C.-Y.; Meethong, N.; Hammond, P. T.; Chiang, Y.-M.; Belcher, A. M. Virus-Enabled Synthesis and Assembly of Nanowires for Lithium Ion Battery Electrodes. *Science* **2006**, *312*, 885−888.
(11) Ni, S.; Li, T.; Lv, X.; Yang, X.; Zhang, L. Designed Constitution of NiO/Ni Nanostructured Electrode for High Performance Lithium Ion Battery. *Electrochim. Acta* **2013**, *91*, 267−274.
(12) Wang, X.; Yang, Z.; Sun, X.; Li, X.; Wang, D.; Wang, P.; He, D. NiO Nanocone Array Electrode with High Capacity and Rate Capability for Li-Ion Batteries. *J. Mater. Chem.* **2011**, *21*, 9988−9990.
(13) Sun, X.; Wang, X.; Qiao, L.; Hu, D.; Feng, N.; Li, X.; Liu, Y.; He, D. Electrochemical Behaviors of Porous SnO_2−Sn/C Composites Derived from Pyrolysis of SnO_2/Poly(vinylidene fluoride). *Electrochim. Acta* **2012**, *66*, 204−209.
(14) Sun, X.; Yan, C.; Chen, Y.; Si, W.; Deng, J.; Oswald, S.; Liu, L.; Schmidt, O. G. Three-Dimensionally "Curved" NiO Nanomembranes as Ultrahigh Rate Capability Anodes for Li-Ion Batteries with Long Cycle Lifetimes. *Adv. Energy Mater.* **2014**, DOI:org/10.1002/aenm.201300912.
(15) Yuan, S.; Zhou, Z.; Li, G. Structural Evolution from Mesoporous α-Fe_2O_3 to Fe_3O_4@C and α-Fe_2O_3 Nanospheres and Their Lithium Storage Performances. *CrystEngComm* **2011**, *13*, 4709−4713.
(16) Li, S.; Xie, W.; Wang, S.; Jiang, X.; Peng, S.; He, D. Facile Synthesis of rGO/SnO_2 Composite Anodes for Lithium Ion Batteries. *J. Mater. Chem. A* **2014**, *2*, 17139−17145.
(17) Zhu, X.; Zhu, Y.; Murali, S.; Stoller, M. D.; Ruoff, R. S. Nanostructured Reduced Graphene Oxide/Fe_2O_3 Composite as a High-Performance Anode Material for Lithium Ion Batteries. *ACS Nano* **2011**, *5*, 3333−3338.
(18) Zhao, Y.; Li, J.; Wang, N.; Wu, C.; Dong, G.; Guan, L. Fully Reversible Conversion Between SnO_2 and Sn in SWNTs@SnO_2@PPy Coaxial Nanocable as High Performance Anode Material for Lithium Ion Batteries. *J. Phys. Chem. C* **2012**, *116*, 18612−18617.
(19) Kong, J.; Yee, W. A.; Wei, Y.; Yang, L.; Ang, J. M.; Phua, S. L.; Wong, S. Y.; Zhou, R.; Dong, Y.; Li, X.; Lu, X. Silicon Nanoparticles Encapsulated in Hollow Graphitized Carbon Nanofibers for Lithium Ion Battery Anodes. *Nanoscale* **2013**, *5*, 2967−2973.
(20) Ma, Y.; Zhang, C.; Ji, G.; Lee, J. Y. Nitrogen-Doped Carbon-Encapsulation of Fe_3O_4 for Increased Reversibility in Li^+ Storage by the Conversion Reaction. *J. Mater. Chem.* **2012**, *22*, 7845−7850.
(21) Lei, C.; Han, F.; Li, D.; Li, W.-C.; Sun, Q.; Zhang, X.-Q.; Lu, A.-H. Dopamine as the Coating Agent and Carbon Precursor for the Fabrication of N-Doped Carbon Coated Fe_3O_4 Composites as Superior Lithium Ion Anodes. *Nanoscale* **2013**, *5*, 1168−1175.
(22) Wang, Y.; Xu, J.; Wu, H.; Xu, M.; Peng, Z.; Zheng, G. Hierarchical SnO_2-Fe_2O_3 Heterostructures as Lithium-Ion Battery Anodes. *J. Mater. Chem.* **2012**, *22*, 21923−21927.
(23) Feng, N.; Qiao, L.; Hu, D.; Sun, X.; Wang, P.; He, D. Synthesis, Characterization, and Lithium-Storage of ZnO-SnO_2 Hierarchical Architectures. *RSC Adv.* **2013**, *3*, 7758−7764.
(24) Qiao, L.; Wang, X.; Qiao, L.; Sun, X.; Li, X.; Zheng, Y.; He, D. Single Electrospun Porous NiO-ZnO Hybrid Nanofibers as Anode Materials for Advanced Lithium-Ion Batteries. *Nanoscale* **2013**, *5*, 3037−3042.
(25) Zeng, W.; Zheng, F.; Li, R.; Zhan, Y.; Li, Y.; Liu, J. Template Synthesis of SnO_2/α-Fe_2O_3 Nanotube Array for 3D Lithium Ion Battery Anode with Large Areal Capacity. *Nanoscale* **2012**, *4*, 2760−2765.
(26) Wu, H.; Xu, M.; Wang, Y.; Zheng, G. Branched Co_3O_4/Fe_2O_3 Nanowires as High Capacity Lithium-Ion Battery Anodes. *Nano Res.* **2013**, *6*, 167−173.
(27) Lee, H.; Dellatore, S. M.; Miller, W. M.; Messersmith, P. B. Mussel-Inspired Surface Chemistry for Multifunctional Coatings. *Science* **2007**, *318*, 426−430.
(28) Kong, J.; Tan, H. R.; Tan, S. Y.; Li, F.; Wong, S. Y.; Li, X.; Lu, X. A Generic Approach for Preparing Core-Shell Carbon-Metal Oxide Nanofibers: Morphological Evolution and Its Mechanism. *Chem. Commun.* **2010**, *46*, 8773−8775.
(29) Kong, J.; Wong, S. Y.; Zhang, Y.; Tan, H. R.; Li, X.; Lu, X. One-Dimensional Carbon-SnO_2 and SnO_2 Nanostructures via Single-Spinneret Electrospinning: Tunable Morphology and the Underlying Mechanism. *J. Mater. Chem.* **2011**, *21*, 15928−15934.
(30) Chen, L. B.; Yin, X. M.; Mei, L.; Li, C. C.; Lei, D. N.; Zhang, M.; Li, Q. H.; Xu, Z.; Xu, C. M.; Wang, T. H. Mesoporous SnO_2 @Carbon Core−Shell Nanostructures with Superior Electrochemical Performance for Lithium Ion Batteries. *Nanotechnology* **2012**, *23*, 035402.
(31) Do, J.-S.; Weng, C.-H. Preparation and Characterization of CoO Used as Anodic Material of Lithium Battery. *J. Power Sources* **2005**, *146*, 482−486.
(32) Zhou, G.; Wang, D.-W.; Li, F.; Zhang, L.; Li, N.; Wu, Z.-S.; Wen, L.; Lu, G. Q.; Cheng, H.-M. Graphene-Wrapped Fe_3O_4 Anode Material with Improved Reversible Capacity and Cyclic Stability for Lithium Ion Batteries. *Chem. Mater.* **2010**, *22*, 5306−5313.
(33) Li, X.; Qiao, L.; Li, D.; Wang, X.; Xie, W.; He, D. Three-Dimensional Network Structured α-Fe_2O_3 Made From a Stainless Steel Plate as a High-Performance Electrode for Lithium Ion Batteries. *J. Mater. Chem. A* **2013**, *1*, 6400−6406.
(34) Sun, Y.-K.; Myung, S.-T.; Park, B.-C.; Prakash, J.; Belharouak, I.; Amine, K. High-Energy Cathode Material for Long-Life and Safe Lithium Batteries. *Nat. Mater.* **2009**, *8*, 320−324.
(35) Kong, J.; Yee, W. A.; Yang, L.; Wei, Y.; Phua, S. L.; Ong, H. G.; Ang, J. M.; Li, X.; Lu, X. Highly Electrically Conductive Layered Carbon Derived from Polydopamine and Its Functions in SnO_2-based Lithium Ion Battery Anodes. *Chem. Commun.* **2012**, *48*, 10316−10318.
(36) Qie, L.; Chen, W.-M.; Wang, Z.-H.; Shao, Q.-G.; Li, X.; Yuan, L.-X.; Hu, X.-L.; Zhang, W.-X.; Huang, Y.-H. Nitrogen-Doped Porous Carbon Nanofiber Webs as Anodes for Lithium Ion Batteries with a Superhigh Capacity and Rate Capability. *Adv. Mater.* **2012**, *24*, 2047−2050.